Permanent Magnet Eddy-Current Losses in 2-D FEM Simulations of Electrical Machines

Simon Steentjes, Stefan Boehmer, and Kay Hameyer

Institute of Electrical Machines, RWTH Aachen University, Aachen D-52056, Germany

The prediction and calculation of eddy current losses occurring in permanent magnets (PMs) of electrical machines is of great interest. Most accurate results are achieved using 3-D finite-element (FE) simulations, which require long computation times and elaborate models. Due to this, 3-D methods are only applied in the final stage of the machine design process. This paper presents different methods to calculate eddy-current losses in PMs by 2-D FE simulations. A radial 2-D FE solver in combination with an axial 2-D FE solver is developed enabling the prediction of the eddy current paths in three dimensions with the associated losses. This approach is applicable to both surface mounted and interior PMs.

Index Terms— **Eddy-currents, losses, numerical simulation, permanent magnet (PM) modeling, PM machines.**

I. Introduction

PERMANENT magnet synchronous machines (PMSMs) are widely applied in electrical machines, the main reasons being: 1) high power density and 2) high efficieny.

Current applications, for instance in electrical and hybrid vehicles, require operation in a wide range of speed. Due to this, next to the mechanical losses, iron and permanent magnet (PM) losses have become increasingly important.

The PM materials are strongly dependent on the temperature [1]. As an example, NdFeB-based PMs have strong thermal constraints for their magnetic coercive field H_c and remanence flux density B_r [1]. Both are degrading very quickly as the temperature of the material increases. This thermal constraint requires that the PM losses are small enough not to heat up the material above the allowed temperatures. Hence, the accurate computation of the occurring losses and the eddy current distribution is indispensable for determining the operation limits or design modification measures.

Due to the rather complex field conditions, in particular due to the finite axial magnet length and an axial segmentation in the circumferential direction, most accurate results are obtained with 3-D finite-element (FE) computations [2]–[5]. Hereby also effects, caused by the slotting of the stator, are considered.

Major drawbacks are the long computation times, as well as exhaustive model building. For these reasons, 3-D FE computations are only partially suitable for the design process of PMSM and are mainly used only at the final stage of the design.

As an alternative, analytical calculation methods are widely used [6]. However, these are mainly limited to surface mounted PM machines [7]–[9] and are derived for special machine designs, thus lacking generality. The 2-D FE computations are then still the main design tools [9]. These can be accurate enough if the materials used in the design are modeled adequately and some 3-D issues are accounted for.

However, modification is required since the basis for 2-D FE simulation is the assumption of a geometry being infinitely long in the axial direction and conducting regions are commonly not considered, unless they are short-circuited at infinity, e.g., rotor bars in asynchronous machines. When calculating eddy-current losses in PMs, the eddy current path is strongly dependent on the geometry of the PM and closes inside one PM. These axial effects are commonly considered using analytical correction factors having disadvantages in considering the changing eddy current field reaction.

In this paper, eddy-current losses are calculated starting from a 2-D FE solution obtained by a 2-D magnetic vector potential solver (2-D-$\mathbf{A}$-ϕ-Solver), which is modified to account for the eddy current path closure inside the PM. This solution is coupled to a modified 2-D electric vector potential solver, which calculates the axial eddy current paths. Therewith, 3-D effects, such as current displacement (skin-effect) and end-effects, as well as the influence of induced eddy currents on the flux density distribution, are accounted for. Hence, eddy-current losses could be calculated using the proposed method inside permanent magnets of different geometric dimensions, i.e., it is applicable for axially long as well as axially short magnets.

This paper is organized as follows. Section II presents the eddy-current loss calculation using either the magnetic vector potential or the magnetic scalar potential. Subsequently, the radial 2-D vector potential solver is modified to account for induced eddy currents closing in the permanent magnet. To include the influence of the axial length of the PM on the eddy current distribution, the radial 2-D-$\mathbf{A}$-ϕ-Solver is coupled to a modified axial 2-D-$\mathbf{T}$-Ω-Solver. Numerical results are discussed, and finally, the conclusions are drawn in Section III.

The presented algorithms have been implemented in the institutes in-house FE-package *iMOOSE* [www.iem.rwth-aachen.de] and have been applied to an example PMSM with surface mounted PMs, as shown in Fig. 1. Detailed geometric parameters of the studied machine can be found in Table I. The 3-D geometry has been generated by extrusion of

Manuscript received May 25, 2014; revised August 26, 2014; accepted September 30, 2014. Date of current version April 22, 2015. Corresponding author: S. Steentjes (e-mail: simon.steentjes@iem.rwth-aachen.de).

Color versions of one or more of the figures in this paper are available online at http://ieeexplore.ieee.org.

Digital Object Identifier 10.1109/TMAG.2014.2362551

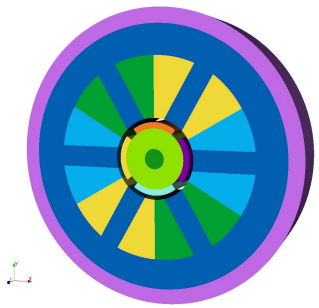

Fig. 1. 3-D geometry of the example PMSM (compare Table I).

TABLE I
GEOMETRIC PARAMETERS

Parameter	Value
Axial Length	10...50 mm
Bore diameter	5 mm
Width of the yoke	15 mm
Conductivity of the PM	$4.73 \cdot 10^5$ S/m^3
Airgap	2 mm
Magnet height	3 mm
Pole angle	82.5 %
Rotor radius	15 mm
Tooth width	10.472 mm

a 2-D geometry. Results of the various 2-D FE solvers are validated using results of a 3-D vector potential solver.

II. PERMANENT MAGNET MODELING

A. General Considerations

Widely applied for simulation of electrical machines is the $\mathbf{A}$-ϕ approach based on the magnetic vector potential $\mathbf{A}$ and the electric scalar potential ϕ [2], [10]

$$\operatorname{curl}(\nu \operatorname{curl}\mathbf{A}) = \mathbf{J}_s - \sigma\,\partial_t\mathbf{A} - \sigma\,\operatorname{grad}\phi + \operatorname{curl}\nu\mathbf{B}_r \tag{1}$$

where ν is the reluctivity of the magnetic material, σ its specific electric conductivity, B_r the remanence of a possible PM modeled as a source term, and J_s the current density of an excitation current.

In combination with the boundary conditions and Gauss' law, a system with two partial differential equations is obtained, which could be solved by a variational approach

$$\sigma \operatorname{div}(\partial_t\mathbf{A} + \operatorname{grad}\phi) = \operatorname{div}\mathbf{J}_s. \tag{2}$$

Hence, the resulting eddy currents $\mathbf{J}_e = -\sigma\,\partial_t\mathbf{A} - \sigma\,\operatorname{grad}\phi$ are solenoidal across whole domain provided that no excitation current density is present.

In contrast to this, the $\mathbf{T}$-Ω approach is based on the magnetic scalar potential Ω and electric vector potential $\mathbf{T}$

$$\operatorname{curl}\left(\frac{1}{\sigma}\operatorname{curl}\mathbf{T}\right) + \frac{1}{\nu}\partial_t\mathbf{T} - \frac{1}{\nu}\partial_t\operatorname{grad}\Omega = -\frac{1}{\nu}\partial_t\mathbf{T}_s - \partial_t\mathbf{B}_r \tag{3}$$

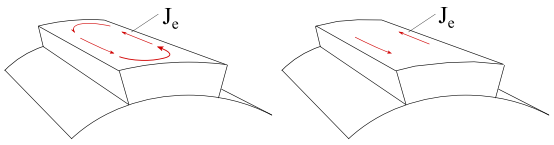

Fig. 2. Left: natural eddy current paths. Right: simplified modeled eddy current paths.

$$\operatorname{div}\left(\frac{1}{\nu}\mathbf{T}\right) - \operatorname{div}\left(\frac{1}{\nu}\operatorname{grad}\Omega\right) = -\operatorname{div}\left(\frac{1}{\nu}\mathbf{T}_s\right) - \operatorname{div}(\mathbf{B}_r). \tag{4}$$

In (3) and (4), $\mathbf{T}_s$ defines an excitation field, which is superimposed on the $\mathbf{T}$-potential. Finally, the eddy-current losses could be calculated by Joule's law.

B. Radial 2-D FE Simulation With Eddy Currents

Commonly, (1) and (2) are simplified for simulations of PM machines by neglecting the induced eddy currents, i.e., setting the specific conductivity to zero ($\sigma \equiv 0$), resulting in

$$\operatorname{curl}(\nu \operatorname{curl}\mathbf{A}) = \mathbf{J}_s + \operatorname{curl}\nu\mathbf{B}_r. \tag{5}$$

Effects of rotational speed (frequency) and excitation current on the magnetic material behavior are accounted for using the corresponding non-linear material characteristic, i.e., $\nu(B^2)$. Losses are calculated during the post-process using the local magnetic flux density waveform. However, this approach is insufficient for eddy current loss calculation in PMs. The eddy current paths close inside the PM itself and the eddy current reaction, as well as the geometry influences the current paths.

To include simple axial eddy currents, closing at infinity, neglecting the electric scalar potential, (5) leads to

$$\operatorname{curl}(\nu \operatorname{curl}\mathbf{A}) + \sigma\,\partial_t\mathbf{A} = \mathbf{J}_s + \operatorname{curl}\nu\mathbf{B}_r \tag{6}$$

with

$$\sigma \operatorname{div}(\partial_t\mathbf{A}) = \operatorname{div}\mathbf{J}_s. \tag{7}$$

Thereby axial eddy currents, closing at infinity, can be calculated in 2-D. The resulting induced eddy current paths are just axial directed: $\mathbf{J}_e = -\sigma\,\partial_t\mathbf{A}$.

Fig. 2 (left) presents a sketch of the natural eddy current path in a PM due to time-varying field excitation in the radial direction and Fig. 2 (right) in contrast to this the simplified version neglecting the end-effects assuming that the magnets are ideally shorted at their axial edges.

As the eddy current paths are closed in one magnet segment, the integral of $\mathbf{J}_e$ over the magnet cross section for each rotor position has to be zero. Deak *et al.* [11] suggest to eliminate the average value $\bar{J}_e$ from the calculated current density. Then, just the alternating current density value J_e remains

$$J_e = J_e - \bar{J}_e \tag{8}$$

where $\bar{J}_e$ corresponds to

$$\frac{1}{\Omega_e}\int_{\Omega_e} \underbrace{-\sigma \cdot \partial_t A_z}_{J_e}\, d\Omega = \bar{J}_e. \tag{9}$$

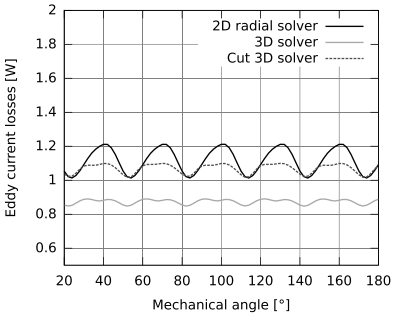

Fig. 3. Evolution of the eddy-current losses (axial length: 40 mm, rotational speed: 3000 min^{-1}).

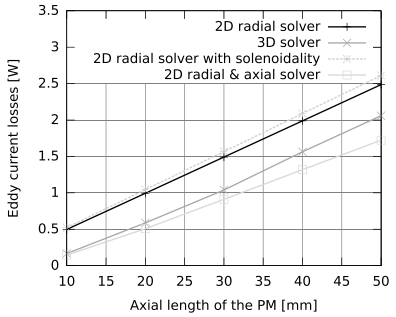

Fig. 4. Comparison of the averaged eddy-current losses (rotational speed: 4000 min^{-1}).

Finally, the eddy-current losses could be calculated as follows:

$$P = l_a \int_{\Omega_e} \frac{(J_e - \bar{J}_e)^2}{\sigma} d\Omega \tag{10}$$

where l_a is the axial length of the PM.

Fig. 3 compares the obtained eddy-current loss at different time instances (axial length: 40 mm, rotational speed: 3000 min^{-1}) to the reference values of the 3-D solver. In addition, results for calculated losses using the eddy currents in the center of the 3-D model are included, i.e., the eddy current density solution from the 3-D solver was cut at half axial length of the PM and the eddy currents have been evaluated on the resulting 2-D solution. It is apparent that the periodicity is the same in all three models, but the amplitude is larger for the 2-D solver. The reason for that is the neglection of the opposing electric field as will be shown subsequently.

Fig. 4 presents the averaged eddy-current losses for different axial length of the PM at a fixed rotational speed of 4000 min^{-1} for the previous (referred to as 2-D radial solver) and other methods presented in this section. The relative error decreases with increasing magnet length. It should be noted that it is essential to have a ratio of axial magnet length and radial magnet width, which is considerably >1 when using this method. These radial 2-D FEM simulations neglect axial effects and assume simplified eddy current paths in the PM as if these were ideally shorted at the edges.

The next step is to use a sufficient approach to ensure the solenoidality of the eddy currents in one PM [12]. Therefore, the electrical scalar potential ϕ is utilized. Hence, the complete equation set of (1) and (2) is used. Induced eddy currents are

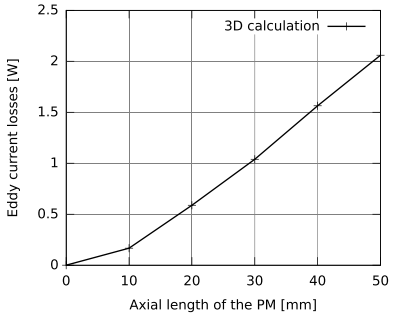

Fig. 5. Averaged values of eddy-current losses at 4000 min^{-1} for various axial length.

calculated according to

$$\mathbf{J}_e = -\sigma \partial_t \mathbf{A} + \sigma \mathbf{E}_o \tag{11}$$

with $\mathbf{E}_o = -\text{grad}\,\phi$ the opposing electric field. In this approach, the voltage drop across each single PM is set to zero to fulfill Gauss' law. Eddy-current losses are finally calculated according to Joule's law

$$P = l_a \int_{\Omega_e} \frac{{J_e}^2}{\sigma} d\Omega \tag{12}$$

where l_a is the axial length. Fig. 4 shows the obtained results, referred to as 2-D radial solver with solenoidality. It is apparent that the error decreases with increasing axial length of the permanent magnet. This is due to the fact that the radial 2-D FE solver includes the reaction field of the axial eddy currents, but not the influence of radial ones. The obtained eddy-current loss at different time instances approaches the reference values.

However, for axial short magnets, large differences for 2-D and 3-D solutions occur. The reason for that is the non-linear relation of axial length of the magnet and its corresponding losses (Fig. 5). Several correction factors [13] to account for this were proposed with limited applicability. Main reason for that is the assumption of rectangular eddy current paths. In case of very wide unsegmented magnets, more than one eddy current loop could be present in the PM due to flux density harmonics.

C. Coupling Radial and Axial 2-D FE Simulation

The aforementioned radial calculation schemes are applicable for PM machines with axially long PMs, i.e., $l_a \gg l_r$. In this section, an approach is presented being able to calculate eddy currents in PMs with small axial length with sufficient accuracy. It is assumed that the influence of the eddy current reaction fields on the magnetic flux density distribution inside the PM is negligible. Furthermore, the eddy currents are assumed to flow in radial slices (Fig. 6). This enables us to treat the axial eddy current problem in a 2-D surface and to consider the skin-effect. As an alternative, a 1-D eddy-current model [14] could serve for this as well. Excited through the solutions of the radial 2-D FE simulation, based on (1) and (2), the eddy current distribution is calculated using an axial electric vector potential solver.

The used modified $\mathbf{T}$ potential solver is based on the $\mathbf{T}$-Ω approach. The reaction of the eddy current field on the magnetic field is neglected, so that the magnetic scalar

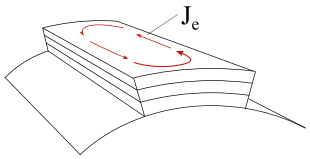

Fig. 6. Division of the PM in various slices.

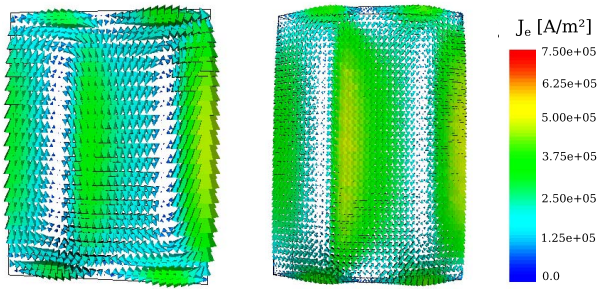

Fig. 7. Comparison of 2-D (left) and 3-D (right) eddy current distribution at a mechanical angle of 14°.

potential Ω remains constant and its gradient vanishes. Equations (3) and (4) can be simplified accordingly

$$\text{curl}\left(\frac{1}{\sigma}\text{curl}\,\mathbf{T}\right)+\frac{1}{\nu}\partial_t\mathbf{T}=-\frac{1}{\nu}\partial_t\mathbf{T}_s-\partial_t\mathbf{B}_r \tag{13}$$

$$\text{div}\left(\frac{1}{\nu}\mathbf{T}\right)=-\text{div}\left(\frac{1}{\nu}\mathbf{T}_s\right)-\text{div}\,(\mathbf{B}_r). \tag{14}$$

The final procedure of the coupled radial and axial 2-D solver is as follows.

1) The PM machine is simulated using the radial 2-D solver, which ensures the solenoidality of the eddy currents in one PM.
2) Meshes for the radial slices (the amount of these is defined by the skin-depth) are automatically generated.
3) The time-varying flux density solution of the radial 2-D solver is used as excitation for the axial solver.
4) Boundary conditions are set, so that no eddy currents occur at the edges.
5) The **T**-Solver calculates the eddy currents in the radial slices.
6) Eddy-current losses can be calculated as

$$P\approx l_s\sum_{j\in\Omega_e}\int_{\Omega_{e,j}}\frac{J_e^2}{\sigma}d\Omega. \tag{15}$$

The results obtained with this approach are included in Fig. 4, referred to as 2-D radial and axial solver. It is apparent that the difference of the 3-D solution and the ones obtained using the axial solver becomes smaller compared with the radial solvers. With decreasing axial magnet length both solutions become very close.

Fig. 7 shows the eddy current paths calculated with the 2-D radial and axial solver (left) and the reference 3-D solver at a rotor position of 14°, i.e., mechanical angle. The distribution is accurately represented, but the amplitudes of the 2-D solution are around 10%–20% smaller in comparison with the 3-D solutions. The reason is that the radial skin-effect is not sufficiently represented using multiple slices. This could be improved using a 1-D eddy-current model [14].

TABLE II
COMPUTATION TIMES: 40 mm, 4000 min^{-1}

Method	Computation time
2D radial solver with solenoidality	254 s
2D radial & axial solver	1372 s
3D solver	8445 s

III. CONCLUSION

This paper presents the sequential improvement of a 2-D FE solver to calculate the induced eddy currents in PMs in electrical machines. The final accuracy is sufficient to calculate the occurring losses in PMs of arbitrary rectangular shape, i.e., axial and radial effects are considered. In addition, the computational effort can be decreased at the same mesh density by six times in comparison with the transient 3-D solver, as shown in Table II. The next steps of this paper will deal with the experimental validation.

REFERENCES

[1] P. Campbell, *Permanent Magnet Materials and Their Application*. Cambridge, U.K.: Cambridge Univ. Press, 1996.
[2] O. Biro and K. Preis, "Finite element analysis of 3-D eddy currents," *IEEE Trans. Magn.*, vol. 26, no. 2, pp. 418–423, Mar. 1990.
[3] K. Yamazaki and Y. Fukushima, "Effect of eddy-current loss reduction by magnet segmentation in synchronous motors with concentrated windings," *IEEE Trans. Ind. Appl.*, vol. 47, no. 2, pp. 779–788, Mar./Apr. 2011.
[4] T. Okitsu, D. Matsuhashi, Y. Gao, and K. Muramatsu, "Coupled 2-D and 3-D eddy current analyses for evaluating eddy current loss of a permanent magnet in surface PM motors," *IEEE Trans. Magn.*, vol. 48, no. 11, pp. 3100–3103, Nov. 2012.
[5] N. Takahashi, H. Shinagawa, D. Miyagi, Y. Doi, and K. Miyata, "Analysis of eddy current losses of segmented Nd–Fe–B sintered magnets considering contact resistance," *IEEE Trans. Magn.*, vol. 45, no. 3, pp. 1234–1237, Mar. 2009.
[6] A. Jassal, H. Polinder, and J. A. Ferreira, "Literature survey of eddy-current loss analysis in rotating electrical machines," *IET Electr. Power Appl.*, vol. 6, no. 9, pp. 743–752, Nov. 2011.
[7] M. Mirzaei, A. Binder, B. Funieru, and M. Susic, "Analytical calculations of induced eddy currents losses in the magnets of surface mounted PM machines with consideration of circumferential and axial segmentation effects," *IEEE Trans. Magn.*, vol. 48, no. 12, pp. 4831–4841, Dec. 2012.
[8] A. Jassal, H. Polinder, D. Lahaye, and J. A. Ferreira, "Comparison of analytical and finite element calculation of eddy-current losses in PM machines," in *Proc. 19th ICEM*, Sep. 2010, pp. 1–7.
[9] W. N. Fu and Z. J. Liu, "Estimation of eddy-current loss in permanent magnets of electric motors using network-field coupled multislice time-stepping finite-element method," *IEEE Trans. Magn.*, vol. 38, no. 2, pp. 1225–1228, Mar. 2002.
[10] K. J. Binns, P. J. Lawrenson, and C. W. Trowbridge, *The Analytical and Numerical Solution of Electric and Magnetic Fields*. Chichester, U.K.: Wiley, 1993.
[11] C. Deak, L. Petrovic, A. Binder, M. Mirzaei, D. Irimie, and B. Funieru, "Calculation of eddy current losses in permanent magnets of synchronous machines," in *Proc. SPEEDAM*, Jun. 2008, pp. 26–31.
[12] A. Belahcen and A. Arkkio, "Permanent magnets models and losses in 2D FEM simulation of electrical machines," in *Proc. 19th ICEM*, Sep. 2010, pp. 1–6.
[13] S. Ruoho, T. Santa-Nokki, J. Kolehmainen, and A. Arkkio, "Modeling magnet length in 2-D finite-element analysis of electric machines," *IEEE Trans. Magn.*, vol. 45, no. 8, pp. 3114–3120, Aug. 2009.
[14] J. Gyselinck, L. Vandevelde, J. Melkebeek, P. Dular, F. Henrotte, and W. Legros, "Calculation of eddy currents and associated losses in electrical steel laminations," *IEEE Trans. Magn.*, vol. 35, no. 3, pp. 1191–1194, May 1999.